ELSEVIER

Cracking Characteristics of Reinforced Steel Fiber Concrete Beams under Short- and Long-Term Loadings

Kiang-Hwee Tan, P. Paramasivam, and Kah-Chai Tan
Department of Civil Engineering, National University of Singapore, Singapore

In this paper, an analytical method for the prediction of maximum crack width in reinforced steel fiber concrete (SFC) beams under short-term loading is first presented. The method accounts for the enhanced cracking strength, restraint against crack growth, and reduced tensile steel strains due to the presence of steel fibers. Based on a correlation analysis, a semiempirical formula for the long-term crack widths in reinforced SFC beams under sustained loads is also proposed. Tests were carried out on 10 beams to investigate the effect of steel fiber content on the cracking characteristics in both the short- and long-term. The results indicated that the use of steel fibers greatly reduced the maximum crack widths in reinforced concrete beams. Good agreement was generally obtained between the analytical predictions and test results. ADVANCED CEMENT BASED MATERIALS 1995, 2, 127–137

KEY WORDS: Beams (support), Cracking characteristics, Crack spacing, Crack widths, Long-term behavior, Reinforced concrete, Steel fibers, Steel fiber concrete, Sustained loading

The addition of steel fibers to conventional reinforced concrete beams greatly improves the cracking strength, restricts the growth of cracks, and reduces the tensile strains in steel reinforcement bars, thereby resulting in smaller crack widths [1–8]. Many studies on the behavior of reinforced steel fiber concrete (SFC) beams under flexural loading, however, were experimental in nature and were aimed at verifying the beneficial effect of steel fibers in controlling deflections and cracks [1–6]. Analytical methods to predict the crack widths in reinforced SFC beams only started to evolve in the late 1980s [7,8].

Address correspondence to: Kiang-Hwee Tan, Department of Civil Engineering, National University of Singapore, 10 Kent Ridge Crescent, Singapore, 0511, Republic of Singapore.
Received May 31, 1994; Accepted October 4, 1994

Ibrahim and Luxmoore [7] proposed a theoretical method that is a modification of Leonhardt's work [9] for the prediction of crack spacings in reinforced SFC beams. The method accounts for the strain in concrete blocks between the cracks. Based on a statistical analysis of test results, a semiempirical formula was derived to calculate the maximum crack width and was found to predict the experimental values reasonably well. However, the formula requires rather lengthy calculations involving many parameters such as the surface deformation of reinforcing bars and the increase of anchorage bond of bars due to fiber inclusion, the latter of which was found to be insignificant by other investigators [10,11]. Al-Ta'an and Al-Feel [8], on the other hand, presented a relatively simpler equation that takes into account variables such as fiber dimensions, volume fraction and type of fibers, and the interfacial bond stress of fibers. The proposed equation also predicted reasonably well the maximum crack widths for the beams reported by the investigators, if the bond strength values of fibers had been appropriately assumed.

The aforementioned studies were, however, confined to short-term loadings. In the present study, a rational approach is presented for the prediction of crack spacings and widths in reinforced SFC beams. The approach accounts for the contribution of steel fibers toward load-carrying capacity across cracks and reduced primary crack heights, and an explicit expression is derived for the calculation of crack widths for beams under short-term loading. Next, based on a correlation analysis, a semiempirical formula is proposed for the determination of the long-term crack widths in reinforced SFC beams under sustained loading. The proposed expressions are compared with the observed crack widths in 10 reinforced SFC beams, 5 of which were tested monotonically to flexural failure and the rest were subjected to sustained loading for a period of over a year.

ISSN 1065-7355/95/$9.50
SSDI 1065-7355(94)00033-A

Advn Cem Bas Mat
1995;2:127–137

Analytical Considerations

Crack Spacing Model

When a reinforced SFC beam is subjected to flexure, cracks will first occur when the extreme tensile fiber stress exceeds the cracking strength of the SFC matrix. These cracks, known as primary flexural cracks, penetrate spontaneously to a level near to the neutral axis after which the force equilibrium and strain compatibility are reestablished. The height of the primary cracks, h_c, may be assumed as equal to the overall beam depth minus the depth of the neutral axis.

According to St. Venant's theory, the formation of a primary crack reduces the tensile stresses on both sides of the crack for a distance approximately equal to h_c. Additional primary cracks are unlikely to occur within these zones of reduced stresses; thus the beam will have primary cracks at spacings of between h_c and $2h_c$. Reinforced SFC beams have been observed to exhibit lower neutral axes or shorter primary cracks, which translates to smaller crack spacings [1,2,4,5,7,12].

After the formation of primary cracks, the tension zone of the beam can be viewed as consisting of a series of tension segments, each lying between two adjacent primary cracks and having a length equal to the primary crack spacing a, as shown in Figure 1. The overall depth of the tension member may be taken as twice the concrete cover to the centroid of the tensile reinforcement.

Further cracks known as secondary cracks will form inbetween the primary cracks if, according to Somayaji and Shah [13], the spacing a is greater than twice the value of the critical transfer length L_t', which is given by:

$$L_t' = k_p \frac{F_{\text{tran}}}{\Sigma o} \tag{1}$$

in which k_p is termed the bond coefficient; Σo is the total perimeter of the reinforcing bars; and F_{tran} is the maximum load transferred to steel fiber concrete from the reinforcing bars through interfacial bond. Because the primary crack spacing has a maximum value of $2h_c$, it follows that secondary crack will occur when $2h_c > 2L_t'$ or $h_c > L_t'$. In this case, the spacing of all cracks including secondary ones would be reduced to between L_t' and $2L_t'$. When $h_c < L_t'$, no secondary cracks will form and the crack spacing in the beam remains between h_c and $2h_c$.

The value of L_t' in eq 1 can be determined by considering a tension segment shown in Figure 2 [14]. At the crack face, the tensile force, F, is carried by the steel bars and steel fibers bridging the cracks. The load from the steel bars is subsequently transferred to the steel fiber concrete through an interfacial bond. At the instant of cracking, it is seen from equilibrium that:

$$F_{\text{tran}} + \sigma_{tu} A_{ce} = A_{ce} \sigma_{cr} \tag{2}$$

where σ_{tu} and σ_{cr} are respectively the postcracking tensile strength and cracking strength of steel fiber concrete. The value of σ_{tu} depends on the ultimate bond strength, length, ratio of cross section to perimeter, orientation factors, and volume fraction of fibers [15]. It is assumed to be independent of the crack opening,

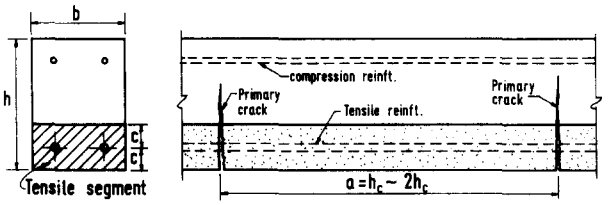

FIGURE 1. Tension segment for crack width calculations.

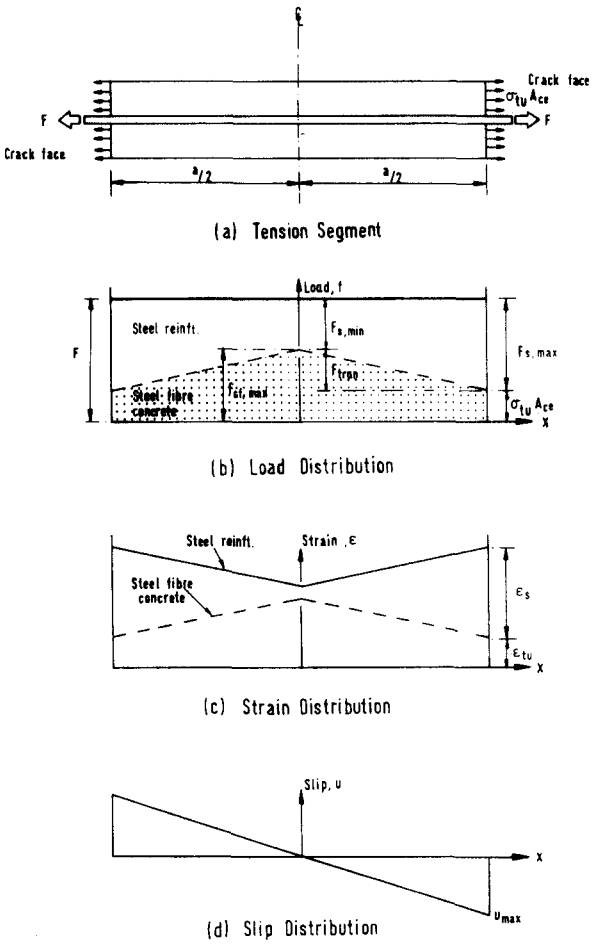

FIGURE 2. Load, strain, and slip distributions in a steel fiber concrete tension segment.

because crack widths found in reinforced SFC beams in flexure are relatively small [2,4]. The term A_{ce} is the effective concrete area and may be expressed as [16]:

$$A_{ce} = 0.8(2c_e b - A_s) \tag{3}$$

with $c_e = (h - d)$; b and h are the breadth and depth of the section respectively; A_s is the total area of steel bars, and d is the effective depth of the beam. The transfer length, L_t', in eq 1 can then be rewritten in view of eqs 2 and 3 as:

$$L_t' = k_p \frac{A_{ce}(\sigma_{cr} - \sigma_{tu})}{\Sigma o} . \tag{4}$$

Short-Term Crack Widths

Referring to Figure 2a, the applied load, F, at the face of a crack, is carried by the steel bars and fibers bridging the crack. The maximum load $F_{s,max}$ in the steel bars occurs at the crack faces, and can be taken as:

$$F_{s,max} = F - \sigma_{tu} A_{ce} \tag{5}$$

This load is assumed to be linearly transferred to the steel fiber concrete through an interfacial bond as shown in Figure 2b. The maximum load in the steel fiber concrete occurs at the center of the segment, and in view of eq 1, is given by:

$$F_{cf,max} = F_{tran} \mid L_{t'} = a/2 + \sigma_{tu} A_{ce}$$

$$= \frac{\Sigma o.a}{2k_p} + \sigma_{tu} A_{ce} \tag{6}$$

The load in reinforcing steel bars, on the other hand, is minimum at the center of the segment and is obtained from equilibrium as:

$$F_{s,min} = F - F_{cf,max} . \tag{7}$$

The stress-strain relationship for steel fiber concrete and steel bar reinforcement may be assumed to be elastic under service load condition. Thus, the total elongation of steel bars, Δ_s, and the corresponding elongation of steel fiber concrete, Δ_{cf}, in half the segment can be obtained from the average strains as (Figure 2b):

$$\Delta_s = \frac{\frac{1}{2}(F_{s,max} + F_{s,min})\frac{a}{2}}{A_s E_s} \tag{8}$$

and

$$\Delta_{cf} = \frac{\frac{1}{2}(F_{cf,max} + \sigma_{tu} A_{ce})\frac{a}{2}}{A_{ce} E_{cf}} \tag{9}$$

that, in view of eqs 5, 6, and 7, can be rewritten as:

$$\Delta_s = \frac{F.a}{2A_s E_s} - \frac{\Sigma o.a^2}{8k_p A_s E_s} - \frac{a.\sigma_{tu} A_{ce}}{2A_s E_s} \tag{10}$$

and

$$\Delta_{cf} = \frac{\Sigma o.a^2}{8k_p A_{ce} E_{cf}} + \frac{a.\sigma_{tu} A_{ce}}{2A_{ce} E_{cf}} . \tag{11}$$

The slip distribution, as shown in Figure 2d, is obtained from the difference between the elongation of the steel bars and the steel fiber concrete. It can be seen from Figure 2d that the slip of steel bars relative to the steel fiber concrete becomes maximum at the crack face, and it can be computed using eqs 10 and 11 for half the segment as:

$$u_{max} = \Delta_s - \Delta_{cf} = \frac{a}{2E_s}\left[f_s - (1 + n\rho_e)\left(\frac{\sigma_{tu}}{\rho_e} + \frac{a}{k_p \phi}\right)\right] \tag{12}$$

where f_s is the applied steel stress that can be computed using the analysis of a cracked reinforced SFC beam section (see Appendix); n is the modular ratio = E_s/E_{cf}; ρ_e is the effective reinforcement ratio = A_s/A_{ce}; and ϕ is the diameter of the steel bars.

The maximum slip calculated using eq 12 represents the slip of the reinforcing bar relative to the SFC matrix at either face of a tension segment of length a. For a reinforced SFC beam under flexural loading, the cracked tension zone is assumed to be composed of multiple tensile segments lying side by side. Hence, the crack width at the level of steel reinforcement is contributed to by the slip of two tension segments at each side of the crack, that is:

$$w_s = 2u_{max} \tag{13}$$

Replacing eq 12 in eq 13 yields the final expression for crack width as:

$$w_s = \frac{a}{E_s}\left[f_s - (1 + n\rho_e)\left(\frac{\sigma_{tu}}{\rho_e} + \frac{a}{k_p \phi}\right)\right]. \tag{14}$$

The maximum crack width in a reinforced SFC beam can be obtained by replacing a in eq 14 with the maximum crack spacing, a_{max}. It is seen from eq 14 that the

Advn Cem Bas Mat
1995;2:127–137

crack width can be reduced not only via a smaller value of f_s, but also by increasing the value of σ_{tu} through the use of an appropriate amount of steel fibers.

Long-Term Crack Widths

Reinforced SFC beams have been observed to exhibit narrower short-term crack width compared to conventionally reinforced concrete beams [1–8]. Thus, assuming a linear correlation, the short-term crack width of a reinforced SFC beam, w_{if}, under a given load can be related to that of a conventional reinforced concrete beam, w_i, as:

$$w_{if} = (1 - k_1 V_f) w_i \tag{15}$$

in which k_1 is an experimental constant that accounts for fiber efficiency factors other than volume fraction of fibers.

On the other hand, the crack widths in a conventionally reinforced concrete beam subjected to sustained loading have been found to increase with time by as much as 100% [17]. The addition of steel fibers could result in an earlier stabilization of crack widths. Thus, the increase in crack width in the long term, w_{lf}, expressed as a ratio of w_{if}, is expected to be smaller for a beam with a higher volume fraction of fibers. That is, for reinforced SFC beams, it may be postulated that:

$$w_{lf} = (k_2 + k_3 V_f) w_{if} \tag{16}$$

that, in view of eq 15, can be rewritten as:

$$w_{lf} = (k_2 + k_3 V_f)(1 - k_1 V_f) w_i \tag{17}$$

where k_2 and k_3 are experimental constants that account for the long-term effects. The constants in eq 17 were established experimentally in this study.

Experimental Investigations

An experimental program was carried out to investigate the material properties and crack widths in 10 reinforced SFC beams in both the short term and long term. The major test variable was the volume fraction of steel fibers. The first group of five beams (beams AF, BF, CF, DF, and EF) were tested monotonically to flexural failure and the others (beams A-50, B-50, C-50, D-50, and E-50) were subjected to sustained loading equal to 50% of the design ultimate load. Four steel test frames were specially fabricated to facilitate flexural creep tests on beams under sustained loads.

Material Properties

Commercially available hooked-end steel fibers were used as fiber reinforcement for all steel fiber concrete mixes. They were 30-mm long (l_f) and 0.5-mm diameter (d_f), with an aspect ratio(l_f/d_f) of 60. The mix proportions for both the plain concrete and the steel fiber concrete were kept at 1:1.5:2.5 by weight of ordinary portland cement, natural sand, and crushed granite of 10-mm nominal size. The water:cement ratio was 0.5 for both mixes. The design strength for the plain concrete was 40 MPa. Sand, aggregates, and cement were mixed dry in the mixer after which water was added. No accelerator or superplasticizer was used. The fibers were dispensed into the wet concrete mix by hand to ensure thorough and uniform dispersion. The amount of steel fibers that were added varied from 0.5% (or 40 kg/m^3) to 2.0% (or 157 kg/m^3) of the volume of concrete.

Six 100-mm cubes, three ϕ150-mm × 300-mm cylinders, and three 100-mm × 100-mm × 400-mm prisms were cast and cured along each group of beams. They were tested on the 28th day for compressive strength, modulus of elasticity, and first crack flexural strength, respectively. The average test values of the material properties are shown in Table 1.

Preparation of Test Specimens

The 10 test beams, each measuring 100 × 125 mm in cross section and 2,000 mm in length, were reinforced with two T10 longitudinal steel bars and two T6 steel bars in the tension and compression zones, at a depth

TABLE 1. Details of test beams

Beam Designation*	Volume Fraction of Fibers, V_f (%)	Cube Strength of Composite, f_{cu} (N/mm^2)	Young's Modulus of Composite, E_{cf} (kN/mm^2)	First Crack Composite Flexural Strength, σ_{cf} (N/mm^2)
AF, A-50	0.0	40.8	29.2	3.35
BF, B-50	0.5	41.2	29.2	4.24
CF, C-50	1.0	42.3	30.2	5.26
DF, D-50	1.5	42.0	30.3	5.33
EF, E-50	2.0	40.8	29.8	6.45

*Beams AF, BF, CF, DF, and EF were loaded monotonically to flexural failure; Beams A-50, B-50, C-50, D-50, and E-50 were subjected to sustained loads equal to 0.5 times the design ultimate load P_u.

from compression face of 99 mm and 24 mm, respectively. Mild steel stirrups (R6) were provided at a spacing of 75 mm throughout the entire length of the beam. The beams were under-reinforced with a tensile steel ratio of 1.60%, compared with a balanced steel ratio of 2.52% for a reinforced concrete beam without fibers.

The beams were compacted using an external table vibrator. They were demoulded after 24 hours and moist-cured for 6 days before being transferred to the vicinity of the test frames and air-cured from the 7th to 28th day under indoor uncontrolled environment. The average ambient temperature and relative humidity were about 27°C and 85%, respectively.

Short-Term Tests

The short-term loading tests were carried out to investigate the influence of steel fiber content on the short-term cracking characteristics of reinforced SFC beams. The five beams, designated AF, BF, CF, DF, and EF (see Table 1), were loaded monotonically to failure at third-points over a simply supported span of 1,800 mm on the 28th day after casting, using a servo-controlled test machine. A typical set-up is shown in Figure 3.

The initiation of cracks in the constant moment zone was detected with the aid of a magnifying glass. The crack spacings and crack widths were measured using a steel ruler with an accuracy of ±0.5 mm and a hand-held microscope with an accuracy of ±0.02 mm, respectively. Four pairs of Demec pins were mounted at a gauge distance of 200 mm across the beam depth on one side at the midspan of the beam for the measurement of concrete strains. The crack widths and spacings at the level of the tensile steel reinforcement in the constant moment zone of 600 mm were measured at a load interval of 1 kN up to failure of the beams, that is, until the crushing of concrete in compression zone had occurred. Concrete strains were measured at appropriate intervals using the Demec gauges.

Long-Term Tests

Five beams, designated A-50, B-50, C-50, D-50, and E-50 (see Table 1), were subjected to sustained loads at the 28th day after casting to investigate the effects of steel fiber content on their long-term cracking characteristics. The beams were simply supported over a clear span of 1,800 mm on the steel frames, as shown in Figure 4. Loads were applied evenly using steel plates and concrete blocks at four points to simulate uniform loading. The sustained loads (chosen to correspond to approximately the characteristic dead load plus half the live load) were equaled to 50% of the design ultimate load in flexure, P_u, which, neglecting the contribution of steel fibers in the tensile zone, was 23.3 kN according to the British Standard BS 8110 [18]. Measurements of crack widths were carried out immediately after the application of loads. The widening of the cracks was monitored regularly for over 1 year.

Test Results and Discussion

The general behavior of the test beams, including the load-deflection and deflection-time relationships were presented separately [19,20]. This paper deals with the cracking characteristics of the beams only.

Cracking Characteristics

Figure 5 shows the cracking patterns at failure for all the test beams subjected to monotonically increasing loads (i.e., beams AF, BF, CF, DF, and EF). It was observed that the presence of fibers in reinforced concrete beams prevented extensive disintegration or crushing of concrete in the compression zone at failure, thus helping the beam to hold together after the maximum load was reached. The cracking patterns were quite similar. The reinforced SFC beams developed new cracks inbetween the primary cracks as fail-

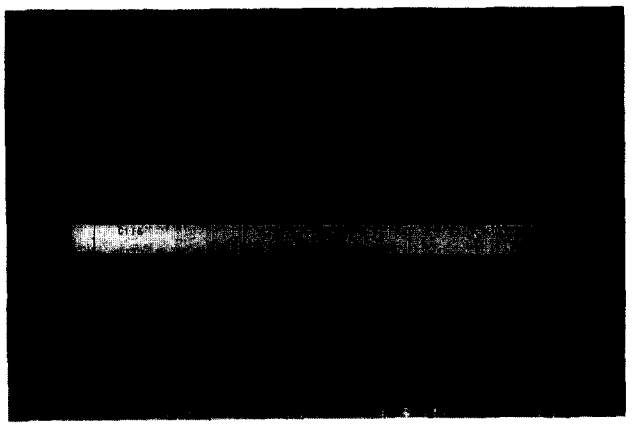

FIGURE 3. Beams subjected to monotonically increasing loads.

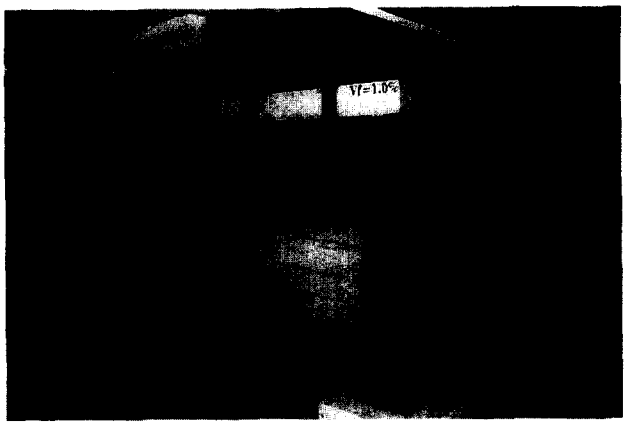

FIGURE 4. Beams subjected to long-term sustained loads.

Advn Cem Bas Mat
1995;2:127–137

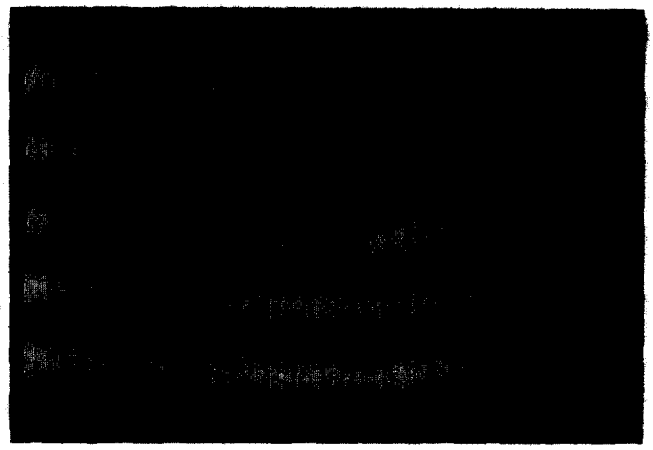

FIGURE 5. Cracking patterns at failure of reinforced steel fiber concrete beams (top to bottom: beams AF, BF, CF, DF, and EF).

ure was approached. The cracks were the result of increased ductility and sustainable beam curvature.

The primary cracks had heights that were shorter in beams with a higher steel fiber content, as shown graphically in Figure 6. This was due to the action of the fibers that restricted the propagation of cracks up the depth of the beams. Similar findings had been reported by other investigators [1,4,7,12].

Crack spacings. The spacings between the primary cracks were not significantly affected by the addition of steel fibers. These primary cracks generally developed at the location of stirrups; thus, the spacings between the cracks closely follow those of the spacings between stirrups. As shown in Figure 7, the spacings between primary cracks varied between one and two times the stirrup spacing, which happened to be of a similar magnitude to the calculated primary crack height (see later section on analytical predictions). The role of stirrups in crack control, especially in the case of those welded to the main reinforcement, requires a separate study [21].

Crack Widths. The maximum crack widths at different load levels from first cracking up to failure for the test beams are shown in Figure 8. It is seen that for a specified load level, reinforced SFC beams exhibited consistently smaller crack widths. In general, the higher fiber content corresponded to the smaller crack width. This was because the steel fibers across cracks contributed in reducing the stress in the tensile steel reinforcement.

Long-term crack widths. Figure 9a shows the increase in maximum crack widths over time for beams subjected to sustained loads. The crack widths for reinforced SFC beams were generally smaller at any point after loading and the higher the fiber content, the smaller the crack width. Figure 9b shows a comparison of the ratio of long-term value to the instantaneous value for the maximum crack width in the beams. The maximum crack widths for reinforced SFC beams (i.e.,

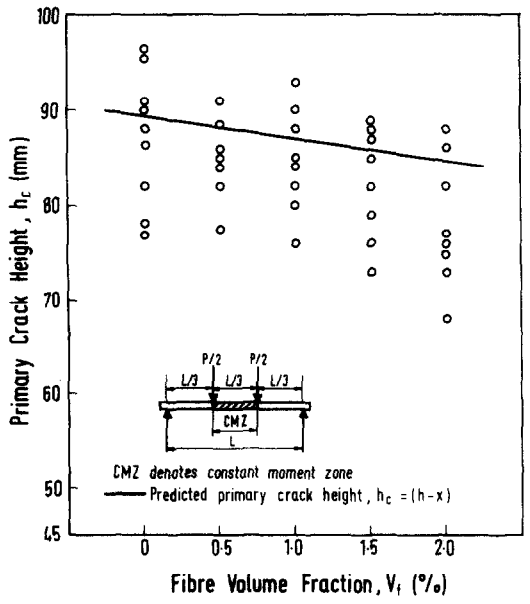

FIGURE 6. Heights of primary cracks at failure of reinforced steel fiber concrete beams.

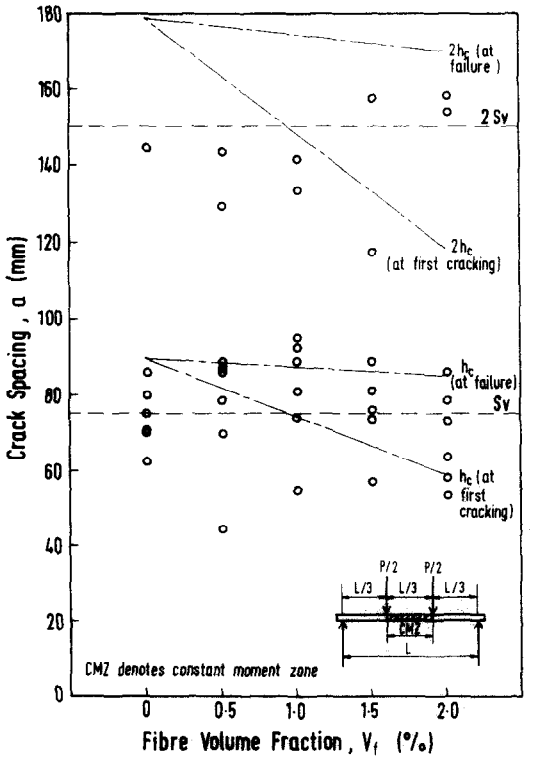

FIGURE 7. Primary crack spacings in reinforced steel fiber concrete beams.

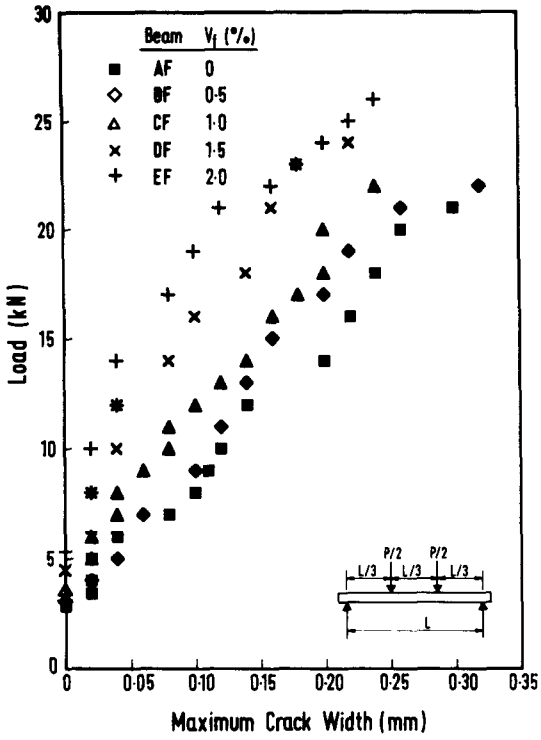

FIGURE 8. Maximum crack widths in reinforced steel fiber concrete beams.

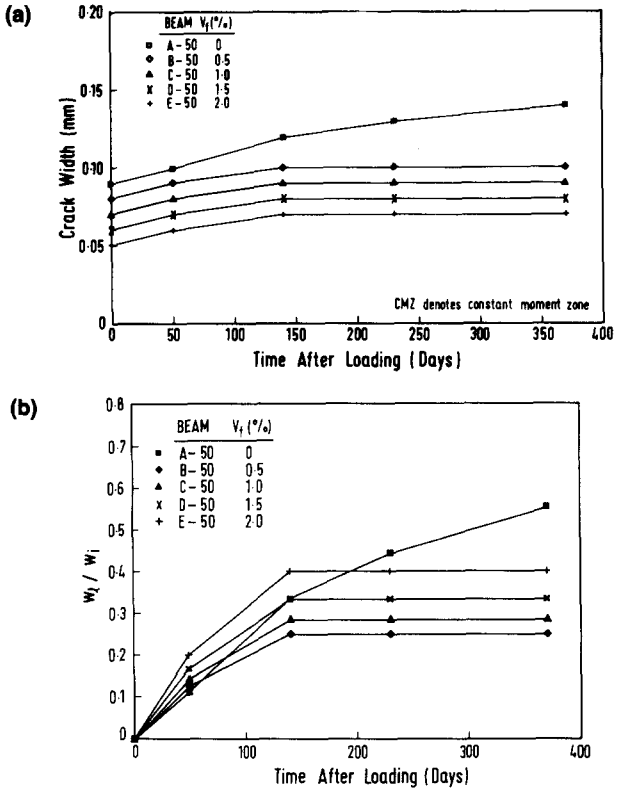

FIGURE 9. (a) Maximum crack widths in reinforced steel fiber concrete (SFC) beams under sustained loads. (b) Ratio of long-term to instantaneous crack widths in reinforced SFC beams.

beams B-50, C-50, D-50, and E-50) stabilized after 140 days whereas that of the conventionally reinforced concrete beam (i.e., beam A-50) was still increasing after 370 days. Thus, it was deduced that fibers helped to prevent the widening of cracks in beams under sustained loading.

Comparison of Test Results with Analytical Predictions

To calculate the crack spacings and, hence, the crack widths, the critical transfer length L_t', for the formation of secondary crack and the primary crack heights h_c first have to be evaluated. The value of L_t' was determined from eq 4 with the first crack flexural strength σ_{cr} obtained experimentally (see Table 1). The post-cracking tensile strength σ_{tu} was evaluated using the equation given by Lim et al. [15], in which the ultimate bond strength of fibers was taken as 5.08 N/mm^2 whereas the bond coefficient k_p was taken as 0.63 mm^2/N [22], assuming that the bond strength of reinforcing bars in concrete is not affected by the addition of steel fibers [10,11].

The primary crack height h_c was calculated as $(h - x)$, where the neutral axis x was computed using the analysis of a cracked section (see Appendix). It is seen from Figure 10 that, in general, the neutral axis depths for reinforced SFC beams were larger than the conventionally reinforced concrete beam, indicating shorter primary cracks. The predicted neutral axis depth was generally in agreement with the experimental results within a reasonable range.

The calculated values of L_t' for all the beams are presented in Table 2 and are compared with the primary crack heights h_c at two levels of loading, namely, just after first cracking and just before failure. It is seen that the primary crack heights h_c were smaller than the critical transfer length L_t' for all the test beams. Thus, theoretically, no secondary cracks are expected and the crack spacings would vary from h_c to $2h_c$. From Figure 6, it is seen that the measured crack spacings in the constant moment zone generally fall within these limits. As previously noted, the average values of h_c coincide with the stirrup spacing s_v of 75 mm; thus, the observed crack spacings also lie between s_v and $2s_v$.

The maximum crack widths at the level of steel reinforcement for the test beams AF, BF, CF, DF, and EF were calculated from eq 14 assuming a maximum crack spacing of $2s_v$ and using tensile steel stress calculated as shown in Appendix A. It can be seen from Figure 11 that the predicted crack widths agree very well with the experimental results, particularly within the service load range. Larger deviation between the pre-

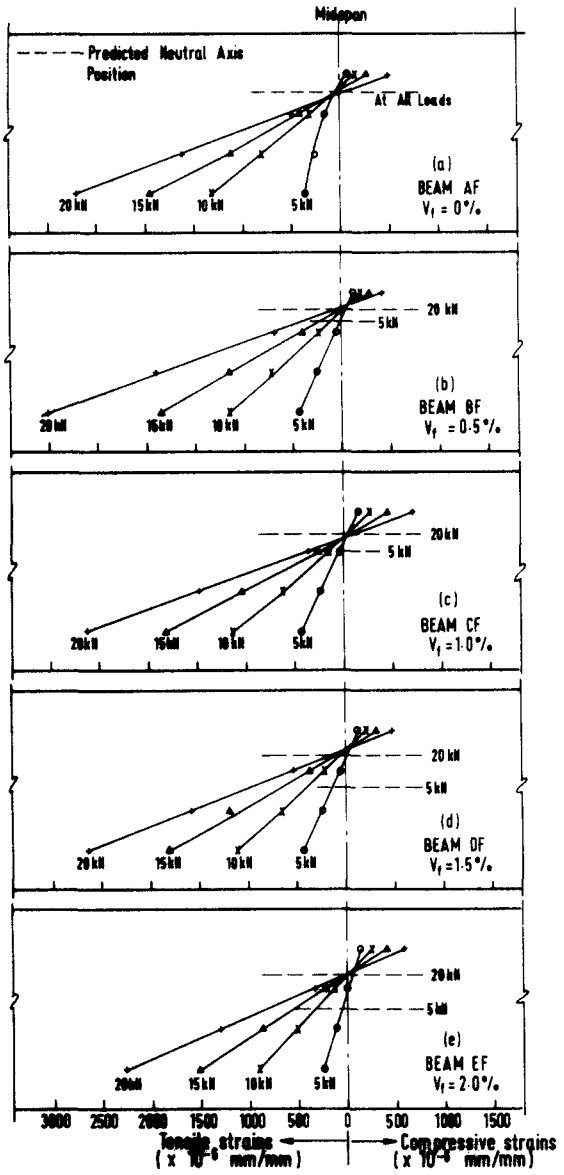

FIGURE 10. Neutral axis locations in reinforced steel fiber concrete beams.

dicted values and test results is observed beyond the service load. This can be attributed to the inelastic behavior of steel fiber concrete and steel reinforcement bars near to failure, contrary to the elastic behavior assumed in the prediction of crack widths.

For the beams subjected to a sustained load of 0.5 P_u, the ratios of the instantaneous crack width in reinforced SFC beams (i.e., beams B-50, C-50, D-50, and E-50) to that in the conventionally reinforced concrete beam (i.e., beam A-50) are shown in Figure 12a. It is seen that the higher the fiber content used, the lower the ratio, confirming the beneficial effect of steel fibers in restricting cracks. Using the results in Figure 12a, the coefficient k_1 in eq 15 was found to be 0.22. Figure 12b shows the relationship between the ratio of the long-term value to the instantaneous value of maximum crack widths and the fiber content of the beams. In general, the ratio of long-term value to instantaneous value of crack width becomes a constant after 140 days for reinforced SFC beams (i.e., where $V_f \neq 0$), reflecting the stabilization of the growth in crack width. A linear regression analysis on the test results of reinforced SFC beams at 370 days yields the values of coefficients k_2 and k_3 in eq 16 as 0.193 and 0.102, respectively, with a correlation factor of 0.98. Substituting the obtained values of k_1, k_2, and k_3 in eq. 17, the long-term crack width in a reinforced SFC beam w_{lf} can be computed from the crack width in a conventionally reinforced concrete beam w_i due to an instantaneous load of the same magnitude, as:

$$w_{lf} = (0.193 + 0.102V_f)(1 - 0.22V_f)w_i \approx (0.19 + 0.10V_f)(1 - 0.22V_f)w_i \quad (18)$$

Conclusions

Within the scope of the study, the following conclusions may be drawn:

TABLE 2. Critical transfer length and primary crack height

Beam Designation	Fiber Volume Fraction, V_f (%)	Critical Transfer Length, L_t' (mm)	Primary Crack Height, h_c (mm)	
			At First Cracking	P^* = 20 kN
AF	0	135.51	89.3	89.3
BF	0.5	137.54	80.9	87.8
CF	1.0	144.82	74.9	86.7
DF	1.5	113.67	64.6	85.1
EF	2.0	125.00	60.8	83.1

P^* = Applied load.

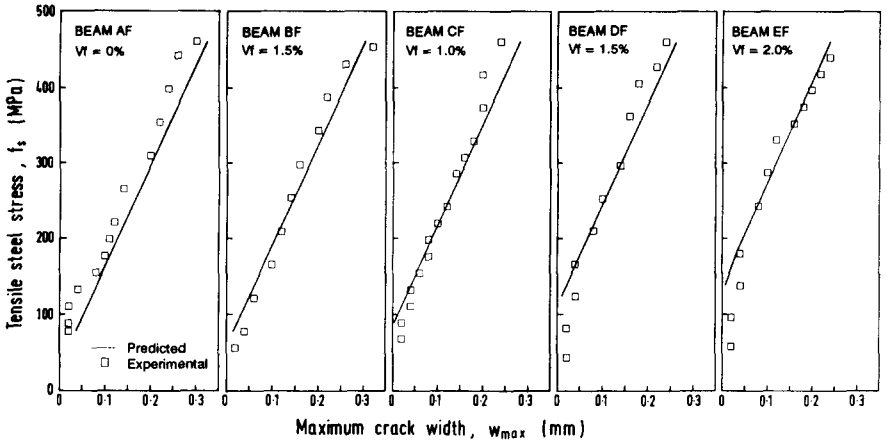

FIGURE 11. Comparison of maximum crack widths in reinforced steel fiber concrete beams with analytical predictions.

1. For beams under monotonically increasing loads, the use of steel fibers resulted in smaller crack widths. For beams under sustained loading, the increase in crack widths was smaller and stabilized at an earlier age for reinforced SFC beams than for conventionally reinforced concrete beams. In both cases, the beneficial effect of fibers increases with the fiber content.
2. A simple, rational method was developed for the prediction of crack widths in reinforced SFC beams under monotonically increasing load. The method was found to give reasonably good predictions, particularly within the service load level.
3. For design purpose, a simple empirical expression has been established to predict the long-term crack widths of reinforced SFC beams from the crack widths in conventionally reinforced concrete beams.

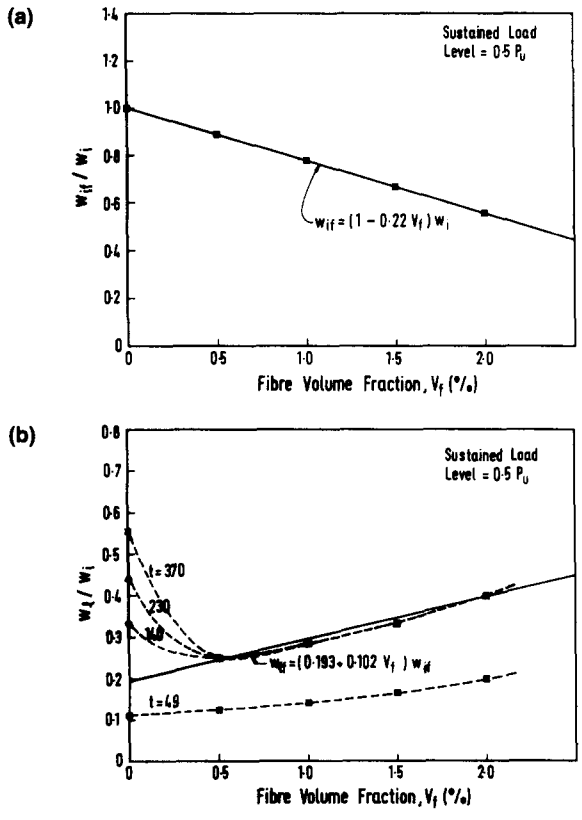

FIGURE 12. (a) Effect of fiber content on instantaneous crack width. (b) Effect of fiber content on long-term crack width.

Acknowledgment

The works upon which this paper is based were supported by the National University of Singapore Research Grants RP880646 and RP900616. The support is gratefully acknowledged.

References

1. Swamy, R.N.; Al-Noori, K.A. In *RILEM Symp. on Fiber Reinforced Cement and Concrete;* The Construction Press Limited: Lancaster, UK, **1975;** pp 187–196.
2. Henager, C.H.; Doherty, T.J. *J. Proc. ASCE.* **1976,** Vol. 12, ST-1, pp 177–188.
3. Kormeling, H.A.; Reinhardt, H.W.; Shah, S.P. *ACI J.* **1980,** *77,* 36—43.
4. Swamy, R.N.; Al-Ta'an, S.A. *ACI J.* **1981,** *78,* 395–405.
5. Bentur, A.; Mindess, S. *Int. J. Cem. Composites Lightweight Concr.* **1983,** *5,* 199–202.
6. Craig, R.J. *Fiber Reinforced Concrete Properties and Applications,* SP-105; American Concrete Institute: Detroit, MI, **1987;** pp 517–564.
7. Ibrahim, O.T.; Luxmoore, A.R. *RILEM Symp.: Developments in Fiber Reinforced Cement and Concrete,* RILEM Technical Committee 49-TFR, Section 8.1; 1986.
8. Al-Ta'an, S.A.; Al-Feel, J.R. *Fiber Reinforced Cements and Concretes: Recent Developments;* Elsevier Science Publishers Ltd.: Essex, UK, **1989;** pp 209–218.

9. Leonhardt, F. *IABSE Surveys* **1977,** S-4/77, 26.
10. Rostasy, F.S.; Hartwich, K. *Int. J. Cem. Composites and Lightweight Concr.* **1988,** *10,* 151–158.
11. Spencer, R.A.; Panda, A.K.; Mindess, S. *Int. J. Cem. Composites Lightweight Concr.* **1982,** 4, 3–17.
12. Swamy, R.N.; Al-Ta'an, S.; Ali, S.A.R. *Concr. Int.* **1979,** American Concrete Institute, *1*(8), 41–49.
13. Somayaji, S.; Shah, S.P. *ACI J.* **1981,** *78,* 217–225.
14. H'ng, S.C. *B. Eng. Dissertation;* Department of Civil Engineering, National University of Singapore, **1990;** 69 pp.
15. Lim, T.Y.; Paramasivam, P.; Lee, S.L. *ACI Struct. J.* **1987,** *84,* 524–536.
16. Desayi, P. *J. ACI* **1976,** *73,* 473–477.
17. ACI Committee 224; *Concr. Int.* **1980,** 2, 35–76.
18. BS 8110; *British Standard Institution* **1985,** 55.
19. Tan, K.H.; Paramasivam, P.; Tan, K.C. *ACI Struct. J.* **1994,** 91(4).
20. Tan, K.H.; Paramasivam, P.; Tan, K.C. *J. Mater. Civil Eng.* **1994,** 6(4).
21. Lee, S.L.; Mansur, M.A.; Tan, K.H.; Kasiraju, K. *J. Struct Eng.* **1989,** *115,* 2645–2660.
22. Lee, S.L.; Mansur, M.A.; Tan, K.H.; Kasiraju, K. *ACI Struct. J.* **1987,** *84,* 481–491.

Appendix: Analysis for a Cracked SFC Section

Referring to Figure A1, a constant stress in the cracked tensile zone is assumed in view of the usually small elastic tensile area and its proximity to the neutral axis. The resultant internal forces on the section are:

compression in SFC, $C_c = 0.5\,\sigma_c bx$ (a)

compression in steel reinforcement, $C_s = E_s\epsilon_s' A_s'$ (b)

tension in SFC, $T_{cf} = \sigma_{tu} b(h - x)$ (c)

tension in steel reinforcement, $T_s = E_s\epsilon_s A_s$ (d)

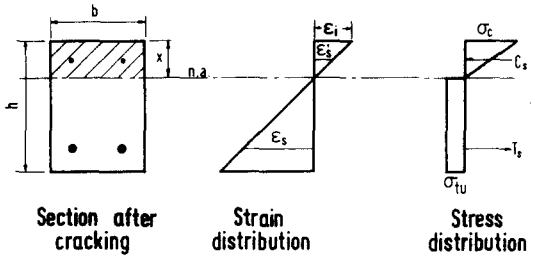

FIGURE A1. Reinforced steel fiber concrete section with corresponding stress and strain distributions.

Equilibrium of forces requires that:

$$C_c + C_s = T_{cf} + T_s \tag{e}$$

Substituting eqs a to d into e and solving for x gives:

$$x = \frac{E_s\epsilon_s A_s - E_s\epsilon_s' A_s' + \sigma_{tu} bh}{0.5E_{cf}\epsilon_c b + \sigma_{tu} b} \tag{A-1}$$

The strains, ϵ_s in the tension reinforcement and ϵ_s' in the compression reinforcement, can be obtained from strain compatibility as:

$$\epsilon_s = \frac{d - x}{x}\epsilon_c \leq \frac{f_y}{E_s} \tag{A-2a}$$

$$\epsilon_s' = \frac{x - d'}{x}\epsilon_c \leq \frac{f_y'}{E_s} \tag{A-2b}$$

where f_y and f_y' are the yield strength of tension and compression reinforcement, respectively. Taking moment about the line of action of the resultant tensile force in the SFC, the internal resisting moment is:

$$M = \frac{1}{2}\sigma_c bx\left(\frac{2}{3}x + \frac{(h - x)}{2}\right) + E_s\epsilon_s' A_s'\left(x - d' + \frac{(h - x)}{2}\right) + E_s\epsilon_s A_s\left(d - x - \frac{(h - x)}{2}\right) \tag{A-3a}$$

By equating the internal resisting moment to the external applied moment, M_a, and replacing ϵ_s and ϵ_s' from eqs A-2a and A-2b, eq A-3a may be rewritten as:

$$\epsilon_c = \frac{M_a}{\frac{1}{2}E_{cf}bx\left(\frac{h}{2}+\frac{x}{6}\right) + E_s\frac{(x-d')}{x}A_s'\left(\frac{x}{2}-d'+\frac{h}{2}\right) + E_s\frac{(d-x)}{x}A_s\left(d-\frac{x}{2}-\frac{h}{2}\right)} \quad \text{(A-3b)}$$

The procedure to determine the neutral axis x is as follows:

1. Assume a value of x.
2. From eq A-3b, calculate ϵ_c.
3. Determine ϵ_s and ϵ_s' from eqs A-2a and A-2b.
4. Calculate the value of x from eq A-1 and compare it with the assumed value of x.
5. Replace the value of x with the calculated value and repeat steps 1 to 4 until the two values converge.